Hazard Avoidance Algorithm for a 3-D Imaging Flash Lidar Utilizing Multi-Frame Super-Resolution Technique

Alexander Bulyshev[1] and Farzin Amzajerdian[2],
[1]*Coherent Applications Inc, Hampton, VA,* [2]*NASA Langley Research Center, Hampton, VA*

Hazard avoidance is important technique for safe landing on space objects. This paper describes a novel approach to safe landing problem by utilizing an onboard Flash Lidar to generate high-resolution elevation maps and applying a threshold-based approach to determine hazardous terrain features and identify safe landing locations.

I. Nomenclature

HDA	Hazard Detection and Avoidance
HAA	Hazard Avoidance Algorithm
GNC	Guidance, navigation, and control
FOV	Field of View
DEM	Digital Elevation Map
SR	Super-Resolution
DoF	Degree of Freedom
FPA	Focal Plane Array
PSF	Point Spread Function

II. Introduction

Flash lidar is recognized as one of the leading sensor technologies for enabling onboard hazard detection and avoidance required by many landing missions including manned and robotic missions to the Moon, Mars, and other planetary bodies. Interest in flash lidar technology stems from its ability to record full 3-D images with a single laser pulse, freezing the scene on every frame by removing all motion of the transmitter/receiver platform. Unlike more conventional topographic imaging lidar systems that generated 3-D images by scanning the laser beam across the scene and measuring the time of arrival for each returned laser pulse, the flash lidar records a full 3-D image frame by illuminating the scene with a single laser pulse and imaging the scene onto one focal plane array (FPA). Each pixel in the FPA takes independent measurements of the lidar pulse time of flight to the target. Therefore, the flash lidar permits much higher frame rates without any blurring or inaccuracies due to platform motion.

Potentials of Flash Lidar technology have been demonstrated through aircraft flight tests and most notably, onboard Morpheus, a terrestrial rocket-powered vehicle.[1-3] Morpheus flight test campaign was conducted at the hazard field specifically constructed for this purpose near the north end of the Shuttle Landing Facility (SLF) runway at NASA Kennedy Space Center (KSC). The hazard field was a 100 m x 100 m area simulating a challenging lunar terrain and consists of realistic hazard features (rock piles and craters) and designated landing areas. Flash lidar operating in closed loop with the vehicle Guidance, Navigation, and Control (GN&C) system, was able to detect the hazards and provide the necessary data for the vehicle to land at the identified safe location. Despite successful outcomes, the Morpheus flight test revealed that flash lidar cannot meet both performance requirements and size and mass constraints of landing vehicles concurrently without further technology advancement.

The hazard detection requirements depend on the landing system design and mission objectives. Many factors must be considered to define the size of surveyed area, minimum detectable hazard size, and the minimum altitude at which the safe landing location is identified and reported to the GN&C system. Lander descent trajectory, divert maneuver capability, and structural properties (clearance from ground, center of gravity, etc.) are some of the considerations for defining the operational requirements of a hazard detection sensor. In order to guide the technology development, a baseline performance for the hazard detection and avoidance sensor has been developed based on robotic and manned lunar lander concepts under consideration. In short, we aim to generate a Digital Elevation Maps (DEMs) each with an approximately 70 m x 70 m area and to detect 30 cm radius hazards before reaching 500 m altitude above ground.

III. 3D Super-Resolution.

Super-resolution is the technique which allows to convert a set of low-resolution images into one high resolution image[4]. Most publications in this area are devoted to solving 2D problems. We have developed and tested a 3D technique for constructing DEMs with sufficiently high resolution meeting the requirements of most landing missions. The SR algorithm consists of three parts:

- 6-DoF image registration, which was developed and implemented based on a modified Lukas&Kanade method
- Back- projected DEM reconstruction method
- Inverse Filter to maximize spatial resolution

Image registration is an important part of the entire process of SR, and it gives a significant advantage to this method. Our version of Lukas&Kanade method provides evolution of camera 6-DoF state vector in the landing site coordinate system. Therefore, when hazard free zones are determined by the HAA algorithm, then the spacecraft position and orientation is known at any given instant and can be directly used by spacecraft GNC system. Image registration algorithm makes registration of the current frame relative to the generated high-resolution DEM by using an iteration of accumulated frames up to that moment.

Back-projection is a procedure to convert range measurement data from Flash Lidar into high- resolution mesh for DEM reconstruction. Back-projection applies to each individual pixel which can be efficiently executed in parallel with other elements of the algorithm. Since back-projection procedure results is the convolution of the high-resolution DEM with some Point Spread Function (PSF), the last step of SR procedure is the PSF calculation and deconvolution. This step is called Inverse Filtering.

First two steps of SR algorithm are applied to each frame individually and use only back-projection DEM accumulated to the current moment. So, they could be processed one by one which makes the whole process suitable for real time implementation. Inverse Filtering should be done only one time for each DEM and it is computationally not expansive.

One of the useful features of the SR algorithm is substituting data from non-responsive pixels from one frame with data from responsive pixels from another frame. Multi frame approach with shifted projections of camera frames on the ground makes this possible. However, if a number of non-responsive pixels are clustered together with a significant size, then full recovery may not be possible. may not be recovered. Such areas of the DEM cannot effectively contribute to identification of hazard-free zones. In order to best utilize all DEM pixels, the SR algorithm computes a Confidence Map, with the same size as SR map, but each cell is filled with the number of hits of the "correct" range measurements. Nonresponsive or bad pixels are not included in the Confidence Map.

IV. Hazard Detection Algorithm

The main goal of the HAA is to find all areas with a circle shape that satisfies the specified safe landing criteria including slope, rocks, and holes. A threshold method is used to discriminated hazardous features and identify hazard-free zones. Two major parameters are essential for hazard determination: average slope and surface roughness. The hazard detection and avoidance algorithm was implemented as a sequence of the following steps:

1. Input Parameters: Radius of the safe area, elevation tolerance, slope tolerance, vehicle state vector (position and attitude), required confidence
2. Define Reference Flat Surface: Establishing a plane in the DEM for calculating terrain surface roughness and slopes
3. Apply hazard thresholds: Detect all features that exceed hazardous height threshold.
4. Identify Safe Locations: Divide the DEM to overlapping circular subsections with a diameter of required safe landing area, apply hazardous slope threshold, and identify safe circular subsections.
5. Select Candidate Landing Locations: Sorting all possible safe subsections, score them based on surface roughness, slope, and number of neighboring safe subsections, provide one or more landing locations to the vehicle.

Figure 1 provides a block diagram of the HAA algorithm

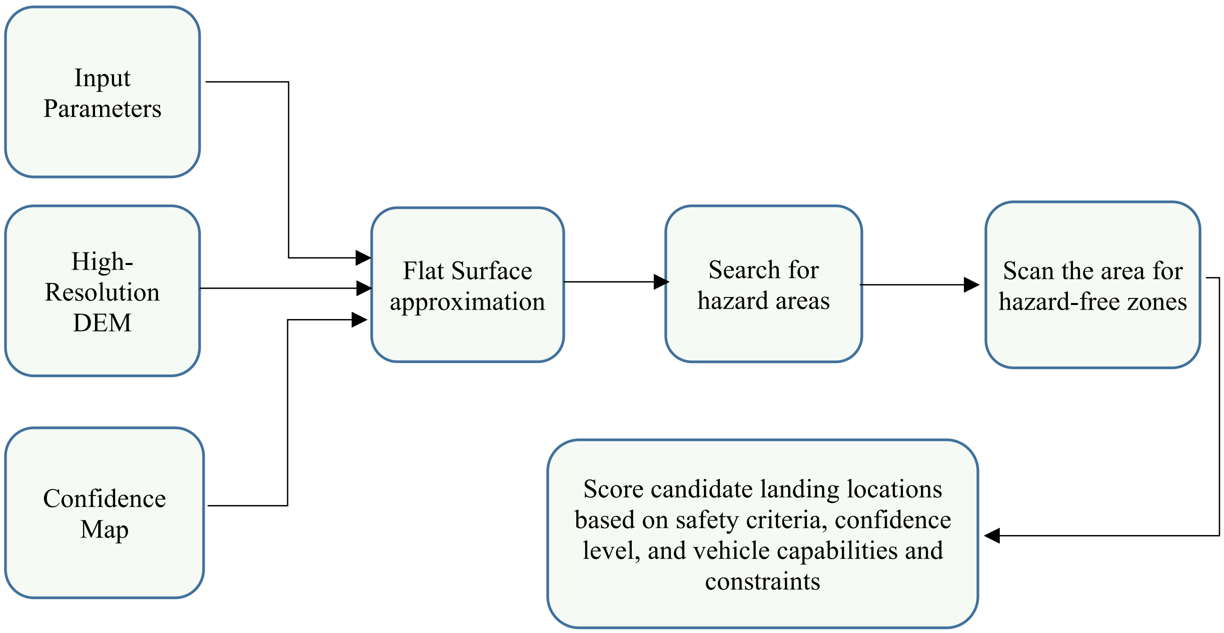

Figure 1. HAA block-diagram.

The smallest spot suitable for safe landing is chosen to be a circle with a given radius. As was claimed before, the main goal of the hazard avoidance algorithm is to find all possible safe landing locations and then sort them based on roughness or slope criteria, confidence level, and vehicle requirements. Therefore, the safe landing area cannot include features with low confidence of accuracy in the restored DEM.

Since DEM is calculated on rectangular equidistant mesh, all inner nodes which are located at list one radius out of area boundaries can be tried as center of safety spot. However, this approach is too computationally expansive. Computational experiments show that some step bigger that distance between 2 neighboring nodes can be used without significant increase in false negative rate of safety spots finding. In general, this step should be an input parameter provided by user.

After all centers coordinates are identified, those areas are tested on roughness and slope criteria. Areas which satisfy the safe landing criteria are labeled as "safe", otherwise it is labeled "hazardous". The result of this step is "Classification Map". All pixels with low confidence labels are automatically "hazardous".

Finally, when all safety landing areas are determined, they are sorted based on surface roughness, the vehicle's divert limitations and preferences, and mission priorities.

V. Gantry Experiment

The algorithm was implemented in Matlab and tested using computer simulated data. As an example, we used DEM model and platform motion profiles from an earlier dynamic experiment conducted at the NASA Langley Gantry facility[5]. Figure 2 shows a general view of the gantry experiment for which the lidar and the associated support instruments were placed in basket suspended by tethers. The basket is lowered by the tethers while some random lateral motions are introduced. The lidar is mounted to the side of the basket such that it has a clear view of a calibrated hazard field constructed under the gantry. Figure 3 shows the calibrated hazard field and the corresponding truth map using the measurements of a laser tracker instrument with millimeter precision.

Figure 2. Dynamic test of Flash Lidar with integrated real-time SR at NASA Langley Gantry facility.

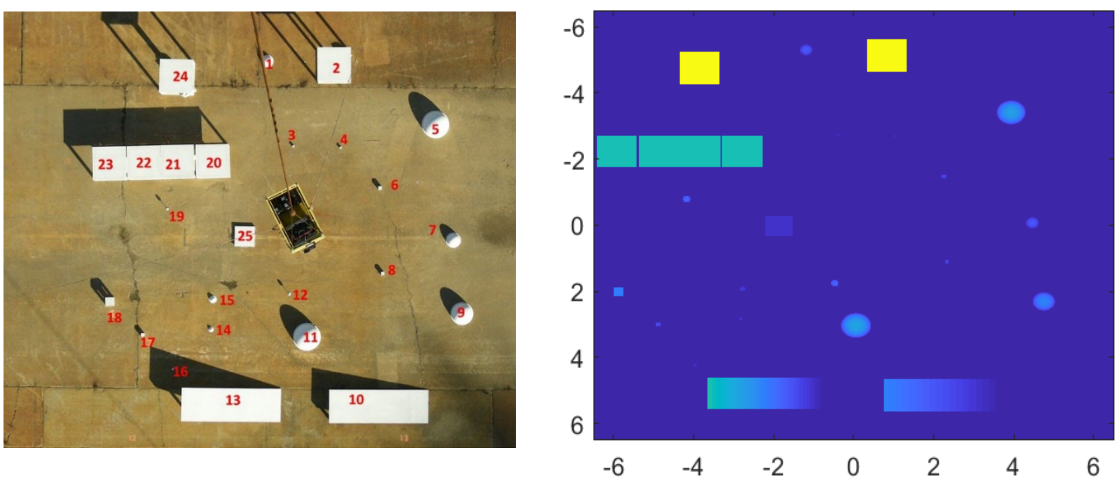

Figure 3. Hazard field (left) and the corresponding DEM model (right) color coded to represent elevation of each object relative to a reference plane.

Figure 4 shows a SR DEM model and the coresponding hazard classification map generated by HAA algorithm. Performance of the HAA algorithm can be quantified as the presentage of correct classification of hazards on a pixel-by-pixel bases. The HAA algorithm was able to identify the hazards with 100% accuracy when applied to the lidar generated SR DEMs. For this exersize, hazards are defined as objects larger than 30 cm in height and slopes greater than 10 degrees and the minimum safe landing area has a 3 meters diameter.

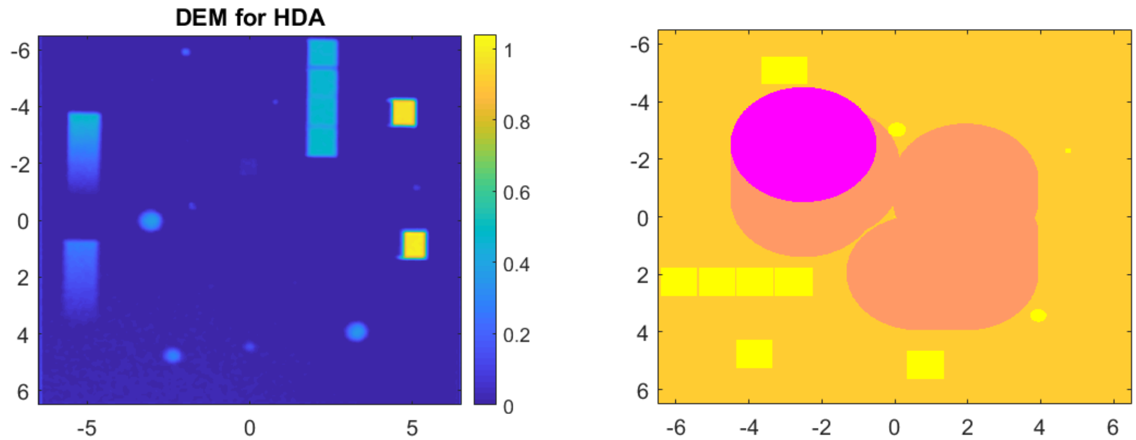

Figure 4. SR DEM (left) and hazard classification map with superimposed hazard free zones meeting safe landing certeria. Brown indicates hazard free area and magenta shows the landing site with minimum roughness.

The same HAA algorithm was then applied to a lidar-generated SR DEM collected during the gantry test. Figure 5 shows the SR DEM generated in real-time by the lidar and the resultant hazard classification map. Unfortunately, there was a rain storm before this test and there were several water puddles in the hazard field which impacted the lidar images. Consequently, most areas with significant water accumulation were classified as hazard by the algorithm. This explains the difference between the hazard classification maps of Figure 4 (DEM model) and Figure 5 (Lidar DEM).

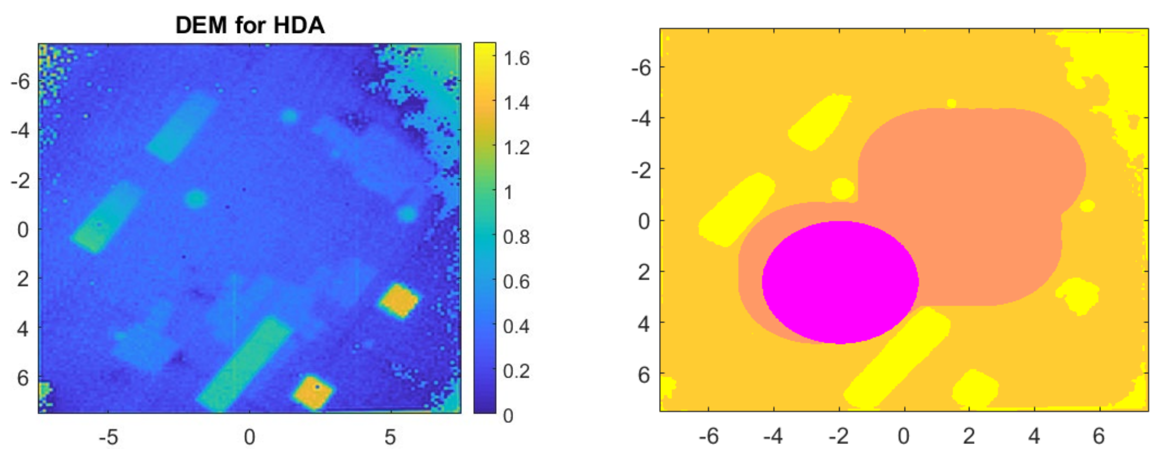

Figure 5. SR DEM (on the left) and results of Hazard Detection Algorithm (right). Brown indicates hazard free area and magenta shows the landing site with minimum roughness..

The gantry test does not simulate the lidar operation in a descent dynamics environment and the hazard field does not represents the actual landing terrain. In order to better assess the performance of the HAA algorithm, the lidar operation was simulated using a nominal lunar landing trajectory and a synthesized lunar terrain and by including the vehicle attitude variations and realistic lidar noise. Initial results showed 98.6% of hazards were detected and 99.7% of safe landing areas were correctly identified. The corresponding false positive and false negative in detection of hazards were 0.05% and 0.01%, respectively. It should be noted that these results are only for one specific descent trajectory and a synthetic lunar terrain to show the potentials of the SR and HAA algorithms developed for the Flash Lidar sensor and cannot be considdred as expected perforamnce for a wide range of lunar landing scenarios.

VI. Conclusion

A hazard detection and avoidance algorithm has been developed as an extension to the Super-Resolution algorithm that had been developed and demonstrated previously for generating high-resolution DEMs using Flash Lidar range image frames. The hazard avoidance algorithm is based on threshold approach and uses surface slope and roughness as primary criteria for generating hazard classification maps. Preliminary computer simulation and application to SR DEMs from a gantry test at NASA Langley Research Center have shown excellent results. However, additional simulation runs, using different vehicle dynamics and terrians, are required to better assess the performance of the Flash Lidar utilizing near real-time SR and HAA algorithms.

References

[1] Carson III, J. M., Robertson, E. A., Trawny, N., and Amzajerdian, F., “Flight Testing ALHAT Precision Landing Technologies Integrated Onboard the Morpheus Rocket Vehicle," Proc. AIAA Space 2015 Conference & Exposition, Pasadena, CA, 2015.

[2] Trawny N, Huertas A., Luna M., Villalpando C., Martin K., Carson III J.M., Johnson A., Restrepo C., Roback V.E., “Flight testing a Real-Time Hazard Detection System for Safe Lunar Landing on the Rocket-powered Morpheus Vehicle,” Proc. of AIAA Science and Technology Forum and Exposition, 2015.

[3] Vincent E. R., Pierrottet D., Amzajerdian F., Barnes B., Hines G., Petway L., Brewster P, Kempton K., and Bulyshev A., “Lidar sensor performance in closed-loop flight testing of the Morpheus rocket-propelled lander to a lunar-like hazard field,” Proc. of AIAA Science and Technology Forum and Exposition, 2015.

[4] Bulyshev A., Amzajerdian F., Roback V.E, Hines G., Pierrottet D., and Reisse R., “Three-dimensional super-resolution: theory, modeling, and field test results,” Appl. Opt. **53**(12), 2583 (2014)

[5] Amzajerdian F, Brewster P., Meadows B., Haq R., Bulyshev B., Shen G., Bieniawski S., Smith B.P., and Kipp D. “Performance of Flash Lidar with real-time image enhancement algorithm for Landing Hazard Avoidance,” AIAA SciTech 2022, San Diego.